

Northwestern University: Report No. NUHEP-713 University of Wisconsin-Madison: Report No. MADPH-00-1203 December 2000

Survival Probability of Large Rapidity Gaps in pp ; $p\bar{p}$; p and \bar{p} Collisions

M. M. Block

Department of Physics and Astronomy,
Northwestern University, Evanston, IL 60208

F. Halzen[†]

Department of Physics,
University of Wisconsin, Madison, WI 53706

Abstract

Using an eikonal analysis, we simultaneously fit a QCD-inspired parameterization of all accelerator data on forward proton-proton and antiproton-proton scattering amplitudes, together with cosmic ray data (using Glauber theory), to predict proton-air and proton-proton cross sections at energies near $\sqrt{s} = 30$ TeV. The p-air cosmic ray measurements greatly reduce the errors in the high energy proton-proton and proton-air cross section predictions, in turn, greatly reducing the errors in the fit parameters. From this analysis, we can then compute the survival probability of rapidity gaps in high energy pp and $p\bar{p}$ collisions, with high accuracy in a quasi-model-free environment. Using an additive quark model and vector meson dominance, we note that the survival probabilities are identical, at the same energy, for p and \bar{p} collisions, as well as for nucleon-nucleon collisions. Significantly, our analysis finds large values for gap survival probabilities, 30% at $\sqrt{s} = 200$ GeV, 21% at $\sqrt{s} = 1.8$ TeV and 13% at $\sqrt{s} = 14$ TeV.

[†]Work partially supported by Department of Energy contract DA-AC02-76-ER02289 Task D.

[†]Work partially supported by Department of Energy grant DE-FG02-95ER40896 and the University of Wisconsin Research Committee with funds granted by the Wisconsin Alumni Research Foundation.

Rapidity gaps are an important tool in new-signature physics for ultra-high energy pp collisions. In this note, we will use an eikonal model to make a reliable calculation of the survival probability of rapidity gaps in nucleon-nucleon collisions.

In an eikonal model [2], we define our (complex) eikonal $\chi(b; s)$ so that $a(b; s)$, the (complex) scattering amplitude in impact parameter space b , is given by

$$a(b; s) = \frac{i}{2} \left[1 - e^{i \chi(b; s)} \right] = \frac{i}{2} \left[1 - e^{-i \chi_I(b; s) + i \chi_R(b; s)} \right] \quad (1)$$

Using the optical theorem, the total cross section $\sigma_{\text{tot}}(s)$ is given by

$$\sigma_{\text{tot}}(s) = 2 \int_0^{\infty} b db \left[1 - \cos(\chi_I(b; s)) \right] e^{-\chi_R(b; s)} \quad (2)$$

the elastic scattering cross section $\sigma_{\text{el}}(s)$ is given by

$$\sigma_{\text{elastic}}(s) = \int_0^{\infty} b db \left[1 - e^{-i \chi_I(b; s) + i \chi_R(b; s)} \right]^2 \quad (3)$$

and the inelastic cross section, $\sigma_{\text{inelastic}}(s)$, is given by

$$\sigma_{\text{inelastic}}(s) = \sigma_{\text{tot}}(s) - \sigma_{\text{elastic}}(s) = \int_0^{\infty} b db \left[1 - e^{-2 \chi_I(b; s)} \right] \quad (4)$$

The ratio of the real to the imaginary part of the forward nuclear scattering amplitude, $\rho(s)$, is given by

$$\rho(s) = \frac{\text{Re} \left[i \int_0^{\infty} b db \left(1 - e^{-i \chi_I(b; s) + i \chi_R(b; s)} \right) \right]}{\text{Im} \left[i \int_0^{\infty} b db \left(1 - e^{-i \chi_I(b; s) + i \chi_R(b; s)} \right) \right]} \quad (5)$$

and the nuclear slope parameter B is given by

$$B = \frac{R}{2} \frac{\int_0^{\infty} b^2 a(b; s) db}{\int_0^{\infty} b a(b; s) db} \quad (6)$$

It is readily shown, from unitarity and eq. (4), that the differential probability in impact parameter space b , for not having an inelastic interaction, is given by

$$P_{\text{no inelastic}} = e^{-2 \chi_I(b; s)} \quad (7)$$

Our even QCD-Inspired eikonal χ_{even} is given by the sum of three contributions, gluon-gluon, quark-gluon and quark-quark, which are individually factorizable into a product of a cross section $\sigma(s)$ times an impact parameter space distribution function $W(b; s)$, i.e.,:

$$\begin{aligned} \chi_{\text{even}}(s; b) &= \chi_{gg}(s; b) + \chi_{qg}(s; b) + \chi_{qq}(s; b) \\ &= i \chi_{gg}(s) W(b; s) + \chi_{qg}(s) W(b; s) + \chi_{qq}(s) W(b; s) \end{aligned} \quad (8)$$

where the impact parameter space distribution function is the convolution of a pair of dipole form factors:

$$W(b; s) = \frac{1}{96} \int_0^b db' K_3(b, b') \quad (9)$$

It is normalized so that $\int_0^{\infty} b db W(b; s) = 1$: Hence, the σ 's in eq. (8) have the dimensions of a cross section. The factor i is inserted in eq. (8) since the high energy eikonal is largely imaginary (the value for nucleon-nucleon scattering is rather small). The total even contribution is not yet analytic. For large s , the even amplitude in eq. (8) is made analytic by the substitution (see the table on p. 580 of reference [3], along with reference [4]) $s \rightarrow s + i = 2$: The quark contribution $\chi_{qq}(s; b)$ accounts for the constant cross section and a Regge descending component ($\chi \sim 1/\sqrt{s}$), whereas the mixed quark-gluon term $\chi_{qg}(s; b)$ simulates diffraction ($\chi \sim \log s$). The gluon-gluon term $\chi_{gg}(s; b)$, which eventually rises as a power law s^p , accounts for the rising cross section and dominates at the highest energies. In eq. (8), the inverse sizes (in impact parameter space)

σ_{qq} and σ_{gg} are to be fitted by experiment, whereas the quark-gluon inverse size is taken as $P_{qq} = \frac{1}{\sigma_{qq}}$. For more detail, see ref.[2].

The high energy analytic odd amplitude (for its structure in s , see eq. (5.5b) of reference [3], with $\beta = 0.5$) that fits the data is given by

$$\sigma_{\text{odd}}^{\text{odd}}(b; s) = \sigma_{\text{odd}} W(b; \sigma_{\text{odd}}); \quad (10)$$

with $\sigma_{\text{odd}} / 1 = P_{\text{odd}} \sqrt{s}$, and with

$$W(b; \sigma_{\text{odd}}) = \frac{\sigma_{\text{odd}}^2}{96} (\sigma_{\text{odd}} b)^3 K_3(\sigma_{\text{odd}} b); \quad (11)$$

normalized so that $\int_0^R W(b; \sigma_{\text{odd}}) d^2b = 1$: Hence, the σ_{odd} in eq. (10) has the dimensions of a cross section. Finally,

$$\sigma_{pp}^{\text{pp}} = \sigma_{\text{even}} + \sigma_{\text{odd}}; \quad (12)$$

We have constructed a QCD-inspired parameterization of the forward proton-proton and proton-antiproton scattering amplitudes [5] which is analytic, unitary, satisfies crossing symmetry and, using a χ^2 procedure, fits all accelerator data [6] of σ_{tot} , nuclear slope parameter B and ρ , the ratio of the real-to-imaginary part of the forward scattering amplitude for both pp and pp collisions; see Fig.1 and Fig.2. In addition, the high energy cosmic ray cross sections of Fly's Eye [7] and AGASA [8] experiments are also simultaneously used [9]. Because our parameterization is both unitary and analytic, its high energy predictions are effectively model-independent, if you require that the proton is asymptotically a black disk. Using vector meson dominance and the additive quark model, we find further support for our QCD fit: it accommodates a wealth of data on photon-proton and photon-photon interactions without the introduction of new parameters [2]. A major difference between the present result, in which we simultaneously fit the cosmic ray and accelerator data, and our earlier result [9], in which only accelerator data are used, is a significant reduction (about a factor of 2.5) in the 1.5% error of our prediction for σ_{pp} at $P_{\text{odd}} \sqrt{s} = 30$ TeV, which results from major reductions in our fit parameters.

The plot of σ_{pp} vs. $P_{\text{odd}} \sqrt{s}$, including the cosmic ray data that have been converted from $\sigma_{\text{p-air}}^{\text{inel}}$ to σ_{pp} , is shown in Fig.1. Clearly, we have an excellent fit, with good agreement between AGASA and Fly's Eye. The overall agreement between the accelerator and the cosmic ray pp cross sections with our QCD-inspired fit, as shown in Fig.1, is striking.

As an example of a large rapidity gap process, we consider the production cross section for Higgs-boson production through W fusion. The inclusive differential cross section in impact parameter space b is given by $\frac{d}{d^2b} = \sigma_{WW \rightarrow H} W(b; \sigma_{qq})$; where we have assumed that $W(b; \sigma_{qq})$ (the differential in impact parameter space quark distribution in the proton) is the same as that of the W bosons.

The cross section for producing the Higgs boson and having a large rapidity gap (no secondary particles) is given by

$$\frac{d_{\text{gap}}}{d^2b} = \sigma_{WW \rightarrow H} W(b; \sigma_{qq}) e^{-2\text{Im} \chi(s; b)} = \sigma_{WW \rightarrow H} \frac{d(\mathcal{P}^2)}{d^2b}; \quad (13)$$

In eq. (13) we have used eq. (4) to get the exponential suppression factor, and have used the normalized impact parameter space distribution $W(b; \sigma_{qq}) = \frac{\sigma_{qq}^2}{96} (\sigma_{qq} b)^3 K_3(\sigma_{qq} b)$, with $\sigma_{qq} = 0.901 - 0.005 \text{ GeV}$, whose error comes from the fitting routine [9].

We now generalize and define $\langle \mathcal{P}^2 \rangle$, the survival probability of any large rapidity gap, as

$$\langle \mathcal{P}^2 \rangle = \int W(b; \sigma_{qq}) e^{-2\text{Im} \chi(s; b)} d^2b; \quad (14)$$

We note that the energy dependence of the survival probability $\langle \mathcal{P}^2 \rangle$ is through the energy dependence of χ , the imaginary part of the eikonal.

For illustration, we show in Fig. 3 a plot of $\text{Im} \chi_{pp}$ and the exponential damping factor of eq. (14), as a function of the impact parameter b , at $P_{\text{odd}} \sqrt{s} = 1.8 \text{ TeV}$. The results of numerical integration of eq. (14) for the survival probability $\langle S^2 \rangle$ at various cm.s. energies are summarized in Table 1. As emphasized earlier, the

C M S. Energy (G eV)	Survival Probability (pp), in %	Survival Probability (pp), in %
63	37.0 0.9	37.5 0.9
546	26.7 0.5	26.8 0.5
630	26.0 0.5	26.0 0.5
1800	20.8 0.3	20.8 0.3
14000	12.6 0.06	12.6 0.06
40000	9.7 0.07	9.7 0.07

Table 1: The survival probability, $\langle \beta^2 \rangle$, in %, for pp and pp collisions, as a function of c.m.s. energy.

errors in $\langle \beta^2 \rangle$ are quite small, due to the fitting parameter errors being very small when we determine the eikonal using both accelerator and cosmic ray data.

Further, we find for the quark component that the mean squared radius of the quarks in the nucleons, $\langle R_{nn}^2 \rangle$, is given by $\langle R_{nn}^2 \rangle = \int b^2 W(b; qq) d^2b = 16 = \frac{2}{qq} = 19.70 \text{ GeV}^{-2}$. Thus, b_{ms} , the r.m.s. in part parameter radius is given by $b_{ms} = 4 = \frac{1}{qq} = 4.44 \text{ GeV}^{-1}$. Inspection of Fig. 3 (1.8 TeV) at b_{ms} shows a sizeable probability for no interaction (e^{-2}) at that typical in part parameter value.

In ref. [2], using the additive quark model, we show that the eikonal P for p reactions is found by substituting $\frac{2}{3}$, $\frac{3}{2}$ into $^{even}(s;b)$, given by eq. (8). In turn, for reactions is found by substituting $\frac{2}{3}$, $\frac{3}{2}$ into $^P(s;b)$. Thus,

$$P(s;b) = i \frac{2}{3} \int_{gg} (s)W(b; \frac{3}{2} \int_{gg}) + \frac{2}{3} \int_{qq} (s)W(b; \frac{3}{2} \int_{qq}) + \frac{2}{3} \int_{qq} (s)W(b; \frac{3}{2} \int_{qq}) ; \quad (15)$$

and

$$(s;b) = i \frac{4}{9} \int_{gg} (s)W(b; \frac{3}{2} \int_{gg}) + \frac{4}{9} \int_{qq} (s)W(b; \frac{3}{2} \int_{qq}) + \frac{4}{9} \int_{qq} (s)W(b; \frac{3}{2} \int_{qq}) ; \quad (16)$$

It can be shown [1], that by an appropriate change of variables, that

$$\langle \beta^2 \rangle = \int W(b; \frac{3}{2} \int_{qq}) e^{-2 \int (s;b)} d^2b \quad (17)$$

where $^P(s;b)$ is given by eq. (15), and

$$\langle \beta^2 \rangle = \int W(b; \frac{3}{2} \int_{qq}) e^{-2 \int (s;b)} d^2b ; \quad (18)$$

where $(s;b)$ is given by eq. (16), are both equal to

$$\langle \beta^{nn} \rangle = \int W(b; \int_{qq}) e^{-2 \int^{even}(s;b)} d^2b \quad (19)$$

where $^{even}(s;b)$ is given by eq. (8). Thus, we have the interesting result that

$$\langle \beta^2 \rangle = \langle \beta^2 \rangle = \langle \beta^{nn} \rangle ; \quad (20)$$

Neglecting the small differences at low energy between pp and pp collisions, we see from eq. (20) that $\langle \beta^2 \rangle$, the survival probability for either nucleon-nucleon, p and collisions, is reaction-independent, depending only on \sqrt{s} , the c.m.s. energy of the collision. We show in ref. [1] that this result is true for any factorization scheme where the eikonal factorizes into sums of $\int (s) W_i(b;)$, with the scaling feature that the product \int_i^2 is reaction-independent not only for the additive quark model that we have employed here. The energy dependence of the large rapidity gap survival probability $\langle \beta^2 \rangle$ calculated from eq. (19) is given in Fig. 4.

This somewhat surprising result can be more readily understood once one realizes that the survival probability is a function of the product 2 and the dimensionless variable $x = \frac{2}{3}qb$. This is most simply seen in a toy model in which the even eikonal is given by

$$e^{i\text{even}}(s;b)_{\text{toy}} = \frac{1}{96} W(b; \frac{2}{3}qb) = \frac{1}{96} \frac{(\frac{2}{3}qb)^3 K_3(\frac{2}{3}qb)}{96} = \frac{1}{96} \frac{x^3 K_3(x)}{96}; \quad (21)$$

and hence,

$$\langle \mathcal{P}^{nn} f_{\text{toy}} \rangle = \frac{1}{96} \int_0^Z e^{-2 \frac{2}{3}qb x^3 K_3(x)} d^2 \mathbf{x}; \quad (22)$$

In our scheme $\frac{1}{96}$ is the same for nucleon-nucleon, p and \bar{p} interactions, since cross sections are multiplied by $\frac{2}{3}$ and $\frac{2}{3}$ for p and \bar{p} , respectively, whereas $\frac{1}{96}$ is divided by $\frac{2}{3}$ and $\frac{2}{3}$. Although x is different for the 3 processes| being qb for nucleon-nucleon, $\frac{3}{2}qb$ for p and $\frac{3}{2}qb$ for \bar{p} it only plays the role of an integration variable and therefore the dependence on the subprocess label disappears. We see from eq. (22) that $S = S(\frac{2}{3}qb)$, which is process-independent. This argument is easily generalized to the full eikonals of eq. (8), eq. (15) and eq. (16).

The physics is now clear. One could be tempted to conclude that the survival probability is larger for p than for pp interactions because there are only 2 quarks in the photon and 3 in the proton to produce additional inelastic collisions filling the gap. And that is true and it is reflected by the factor 2/3 change in the cross section. This is not the whole story, however. In the eikonal model, the inverse transverse size of the 2-quark system (photon) is larger than that of the proton (the $\frac{3}{2}$ factor) and the two effects compensate. Therefore, we have the same $\langle \mathcal{P}^f \rangle$ for all processes.

We have been able to calculate the survival probability $\langle \mathcal{P}^f \rangle$ to a high degree of accuracy by using an eikonal that has been found by fitting both accelerator and cosmic ray data over a very large energy range which includes the LHC energy. Our numerical results are considerably larger than other calculations [10, 11, 12]. In the case of ref. [10] and ref. [12] it is probably due to their using a Gaussian probability distribution in impact parameter space, whereas our distribution, $W(b; \frac{2}{3}qb) = \frac{1}{96} (\frac{2}{3}qb)^3 K_3(\frac{2}{3}qb)$ which is the Fourier transform of the square of a dipole distribution, has a long exponential tail e^{-b} , significantly increasing the probability of survival. In the case of ref. [11], the authors determine the parameters for their minijet model using only the Tevatron results. Our large values are more in line with the earlier predictions of Gotsman et al [13] for what they called Regge and Lipatov1 and Lipatov2 models, although with somewhat different energy dependences than that shown in Table 1. The color evaporation model of Eboviet al [14] gives somewhat larger values than our calculation, but again with a different energy dependence. Most recently, Khoze et al [15], using a two-channel eikonal, have calculated the survival probabilities for rapidity gaps in single, central and double diffractive processes at several energies, as a function of b , the slope of the Pomeron-proton vertex. For double diffraction, they have a large range of possible parameters. Choosing $2b = 5.5 \text{ GeV}^{-2}$ (corresponding to the slope of the electromagnetic proton form factor), they obtain $\langle \mathcal{P}^f \rangle = 0.26, 0.21$ and 0.15 at $\sqrt{s} = 0.54, 1.8$ and 14 TeV , respectively. These survival probabilities are in excellent agreement with our values given in Table 1. However, their calculations for other choices of $2b$ and for single and central diffractive processes do not agree with ours, being model-dependent, with their results varying considerably with their choice of parameters and model.

We see that there is a serious model dependence, both in the size of the survival probabilities and in their energy dependence. Further, until now, there has been no estimates for gap survival probabilities for p and \bar{p} reactions. Thus, we hope that our quasimodel-independent fit to experimental data on pp and $p\bar{p}$ total cross sections, values and nuclear slopes B , over a large energy range, $\sqrt{s} = 15 \text{ GeV}$ to $30,000 \text{ GeV}$, provides a reliable quantitative estimate of the survival probability $\langle \mathcal{P}^f \rangle$ as a function of energy, for both $pp, p\bar{p}, p$ and \bar{p} collisions. The fact that our estimates of large rapidity gap survival probabilities are independent of reaction, thus being equal for nucleon-nucleon, p and \bar{p} processes| the equality surviving any particular factorization scheme| has many interesting experimental consequences.

References

- [1] M . M . B lock and A . B . K aidalov, "Consequences of the Factorization Hypothesis in pp; pp; p and Collisions", e-Print Archive: hep-ph/0012365, Northwestern University preprint N J H E P No. 712, Nov. 2000.
- [2] M . M . B lock et al, e-Print Archive: hep-ph/9809403, Phys. Rev. D 60, 054024 (1999).
- [3] M . M . B lock and R . N . C ahn, Rev. Mod. Phys. 57, 563 (1985).
- [4] Eden, R . J., "High Energy Collisions of Elementary Particles", Cambridge University Press, Cambridge (1967).
- [5] M . M . B lock et al, Phys. Rev. D 45, 839 (1992).
- [6] We have now included in the accelerator data the new E-811 high energy cross section at the Tevatron: C . A vila et al, Phys. Lett. B 445, 419 (1999).
- [7] R . M . B altrusaitis et al, Phys. Rev. Lett. 52, 1380 (1984).
- [8] M . H onda et al, Phys. Rev. Lett. 70, 525 (1993).
- [9] In an earlier communication, the accelerator data alone were fitted. Using the parameters from that fit, we then made a separate fit of the cosmic ray data to the value of k ; see M . M . B lock et al, e-Print Archive: hep-ph/9908222, Phys. Rev. Lett. 83, 4926 (1999). In this work, we make a simultaneous fit of the accelerator and the cosmic ray data, a much more complicated and very lengthy numerical analysis but also a much superior physical analysis, resulting in greatly reduced errors in our predictions of high energy values of σ_{pp} and $\sigma_{p\text{ air}}^{\text{inel}}$; see M . M . B lock et al, e-Print Archive: hep-ph/0004232.
- [10] E . G otsm an, E . Levin and U . M aor, Phys. Lett. B 438, 229 (1998); e-Print Archive: hep-ph/9804404.
- [11] R . S . F letcher and T . Stelzer, Phys. Rev. D 48, 5162 (1993).
- [12] J . D . B jorken, Phys. Rev. D 47, 101 (1993).
- [13] E . G otsm an, E . Levin and U . M aor, Phys. Lett. B 309, 199 (1993).
- [14] O . J . P . E boli, E . M . G regores and F . Halzen, Phys. Rev. D 61, 034003 (2000).
- [15] V . A . K hoze, A . D . M artin and M . G . R yskin, e-Print Archive: hep-ph/0007359.

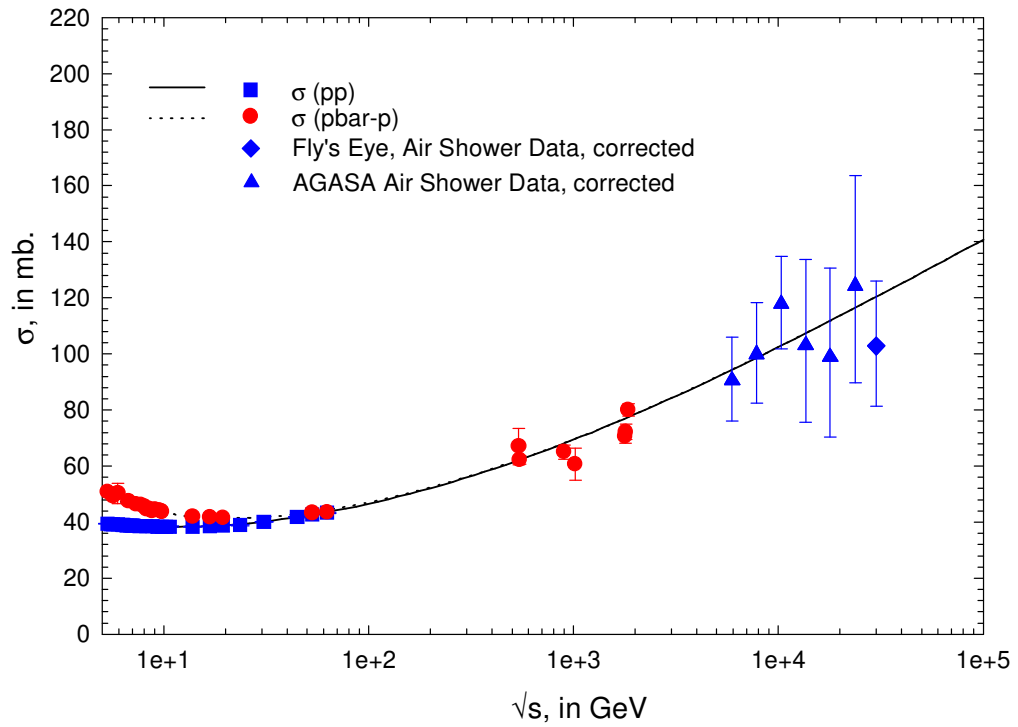


Figure 1: The fitted σ_{pp} and $\sigma_{p\bar{p}}$, in mb vs. \sqrt{s} , in GeV, for the QCD-inspired fit of total cross section, B and σ_{pp} for both pp and $p\bar{p}$. The accelerator data (squares are pp and circles are $p\bar{p}$) and the cosmic ray points (diamond, Fly's Eye and triangles, AGASA) have been fitted simultaneously. The cosmic ray data that are shown have been converted from $\sigma_{p\text{air}}^{\text{inel}}$ to σ_{pp} .

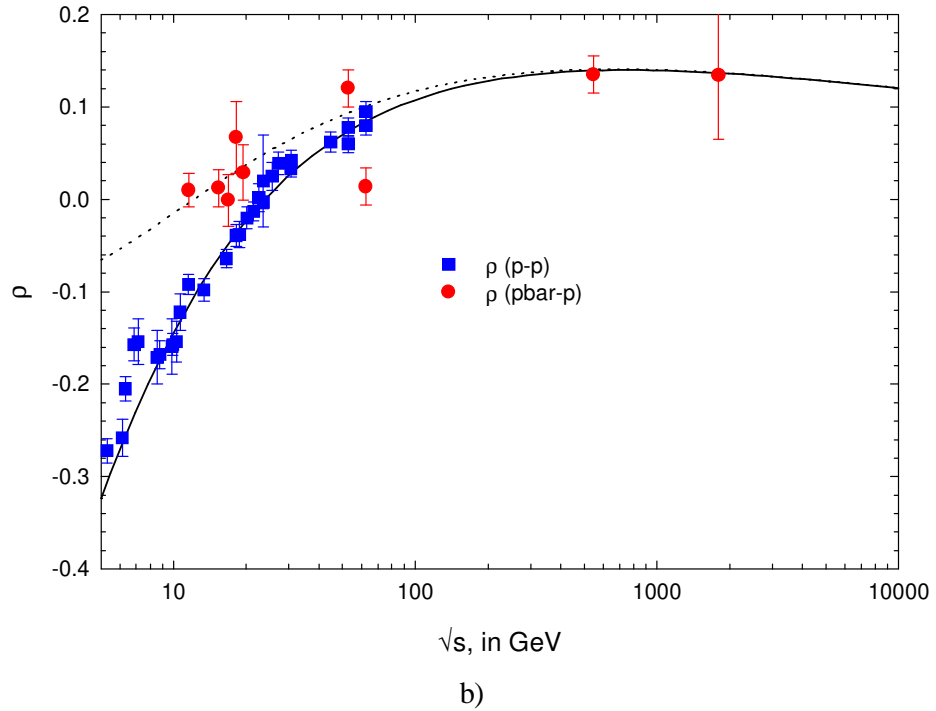
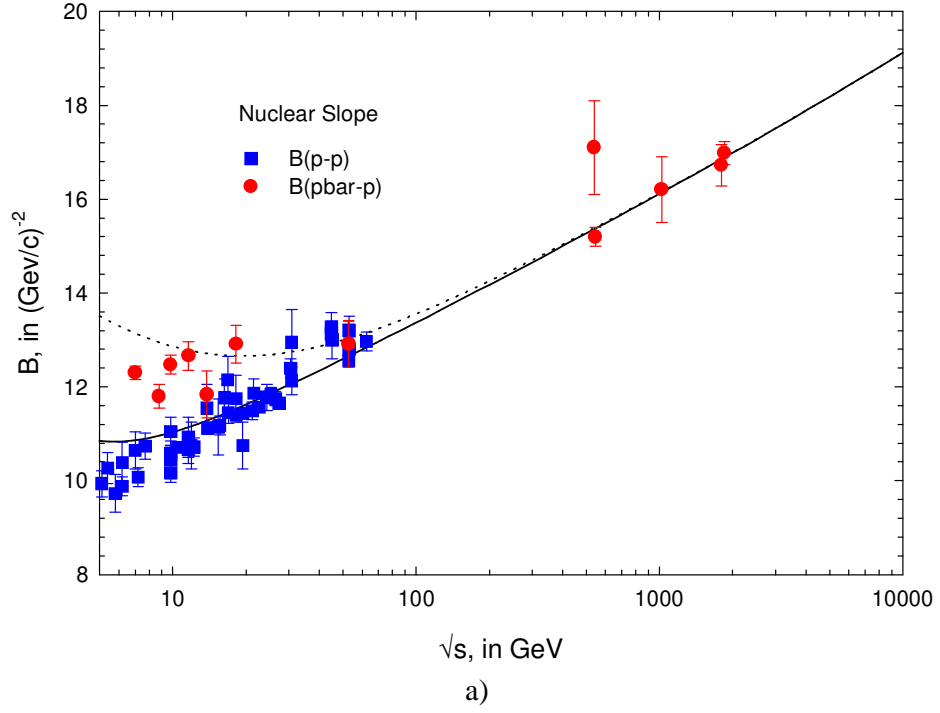


Figure 2: The fitted values for the nuclear slope parameters B_{pp} and $B_{p\bar{p}}$, in $(\text{GeV}/c)^2$ vs. \sqrt{s} , in GeV , for the QCD-inspired fit are shown in (a). In (b), the fitted values for ρ_{pp} and $\rho_{p\bar{p}}$ are shown.

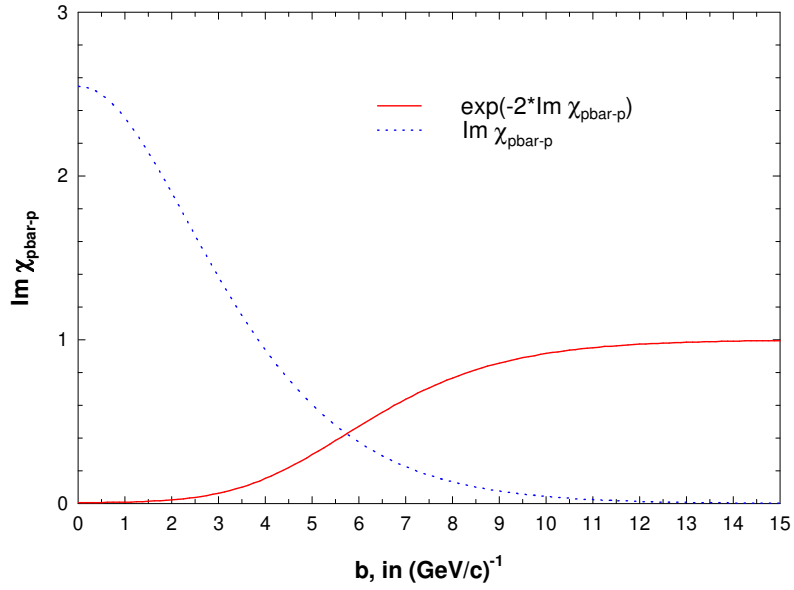


Figure 3: A plot of the eikonal $\text{Im } \chi_{p\bar{p}-p}$ and the exponential damping factor $e^{-2 \text{Im } \chi_{p\bar{p}-p}}$ for pp collisions, at $\sqrt{s} = 1.8 \text{ TeV}$ vs. the impact parameter b , in $(\text{GeV}/c)^{-1}$.

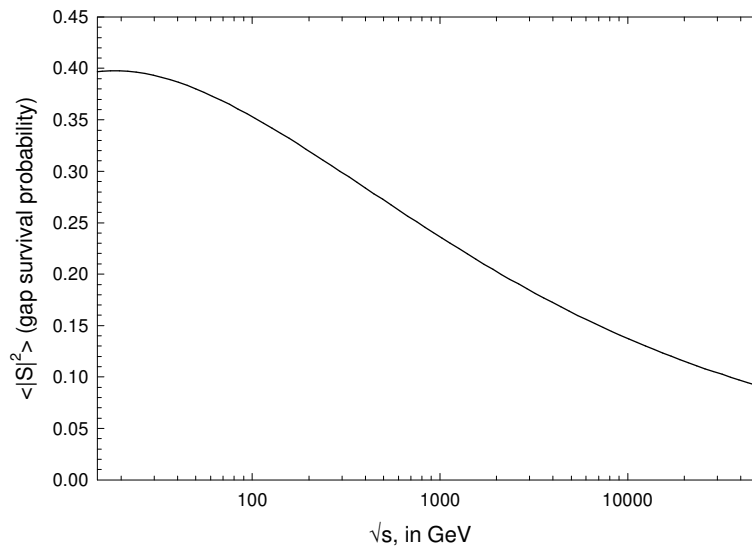


Figure 4: The energy dependence of $\langle |S|^2 \rangle$, the large rapidity gap survival probability vs. \sqrt{s} , in GeV.